International Journal of
Turbomachinery
Propulsion and Power

MDPI

Article

The Effect of Hot Streaks on a High Pressure Turbine Vane Cascade with Showerhead Film Cooling †

Giovanna Barigozzi, Silvia Mosconi, Antonio Perdichizzi and Silvia Ravelli *

Department of Engineering and Applied Sciences, University of Bergamo, 24044 Dalmine, Italy; giovanna.barigozzi@unibg.it (G.B.); silvia.mosconi@hotmail.it (S.M.); antonio.perdichizzi@unibg.it (A.P.)

* Correspondence: silvia.ravelli@unibg.it; Tel.: +39-035-205-2346

† This paper is an extended version of our paper in Proceedings of the European Turbomachinery Conference ETC12, 2017, Paper No. 44.

Academic Editor: Tony Arts
Received: 10 May 2017; Accepted: 6 September 2017; Published: 13 September 2017

Abstract: Hot streak migration in a linear vane cascade with showerhead film cooling was experimentally and numerically investigated at isentropic exit Mach number of Ma_{2is} = 0.40, with an inlet turbulence intensity level of Tu_1 = 9%. Two tangential positions of the hot streak center were taken into account: 0% of pitch (hot streak is aligned with the vane leading edge) and 45% of pitch. After demonstrating that computations correctly predict hot streak attenuation through the vane passage with no showerhead blowing, the numerical method was used to investigate hot streak interaction with showerhead film cooling, at blowing ratio of BR = 3.0, corresponding to a coolant-to-mainstream mass flow ratio of MFR = 1.15%. The effects of mixing and coolant interaction on the hot streak reduction were interpreted under the light of the superposition principle, whose accuracy was within 12% on the leading edge region, in the central section of the vane span.

Keywords: hot streak; first stage vane; showerhead film cooling

1. Introduction

In a first stage nozzle vane cascade, the inlet temperature field contains spanwise and pitchwise gradients resulting from combustor exit conditions. These distortions in temperature, the so-called hot streaks, are related to the finite number of combustors upstream of the high-pressure turbine, to their geometry and to the presence of dilution air jets and discrete injection of fuel within the combustor. Hot streaks coming from the combustor do not modify the streamline flow pattern inside the vane passage, and secondary flows either [1], except when combined with inlet total pressure distortions [2,3]. Conversely, hot streaks can have a significant impact on high-pressure vane heat transfer. Povey et al. [4] and Qureshi et al. [5] demonstrated that the heat transfer rate on the suction side of the vane increases, over the uniform inlet temperature results, when hot streaks are aligned with the leading edge. Conversely, the heat transfer rate over the vane pressure side was found to be insensitive to inlet temperature non-uniformities.

The abovementioned studies refer to non-uniform inlet temperature profiles in solid vane cascades. However, it is important to understand the interaction of hot streaks with film cooling. First of all, hot streaks are critical for maximizing the cooling system performance, as the cooling system would be designed for a mainstream temperature higher than the mass mean gas temperature. In a first stage nozzle guide vane, depending on the position of the hot streak with respect to the leading edge, a greater amount of coolant may be required to keep the vane surface temperature at acceptable levels. Moreover, hot streak interaction with the vane row and coolant can alter the temperature distribution at the rotor inlet, and consequently its cooling requirement.

The migration of radial temperature profiles through a turbine stage was examined by Mathison et al. with and without cooling flows [6]. In the absence of cooling, mixing through the vane passage reduces the temperature peak and redistributes the warm flow to the outer span. With the introduction of cooling, a nearly uniform reduction in temperature was measured from the inlet to the exit of the stage. Ong and Miller performed an experimental validation study on an engine high pressure turbine stage with representative inlet hot streak and vane coolant conditions [7]. Once it has been established that the computations predict well the temperature field at the vane and rotor exit, the potential for using the coolant injected from the vane row to perform a secondary cooling function in the rotor row was numerically assessed. Similarly, the study by Basol et al. was focused on the effect of hot streak on rotor heat load: it was shown that shifting the hot streak towards the stator pressure side increases the heat load on the blade around the midspan [8]. Regina et al. confirmed that heat load distributions approaching components downstream of a combustor can be controlled by means of shaping the inlet temperature distortion to the turbine [9].

When dealing specifically with cooled vane cascades, the attenuation of a hot streak as it travels across the passage was experimentally quantified by Jenkins et al., under the combined effect of high turbulence and film cooling [10]. It was found that high turbulence levels and full coverage film cooling, including showerhead, suction side, and pressure side film cooling holes, are responsible for a peak hot streak temperature reduction up to 74% relative to the upstream conditions. A further step in the analysis consisted in evaluating the capability of additive superposition in predicting hot streak reduction due to film cooling, starting from independent hot streak and film cooling results [11]. Errors in predicting the peak of the cooled hot streak were below 20%. Another upgrade in the study of film cooled high pressure vanes with non-uniform inlet conditions was proposed by Griffini et al. [12]. They employed the conjugate heat transfer analysis to establish that the hot streak alignment with the leading edge makes average and local temperature peaks increase on both the suction and pressure side of the vane, with respect to the passage-aligned configuration.

The present paper reports on hot streak migration in a vane cascade with showerhead cooling holes, for two different relative clocking positions between hot streak and airfoil. Main assumptions are the following: the number of stator vanes is multiple of the number of fuel nozzles; the inlet flow is purely axial. The decay in the strength of the hot streak across the passage was experimentally and numerically evaluated, with and without the showerhead film cooling. The goal was to determine the film cooling contribution to hot streak reduction. Moreover, the impact of hot streak on vane surface temperature was quantified with particular attention to the leading edge region, with the aim of verifying the applicability of the superposition method.

2. Experimental Setup

Tests were performed in a suction-type wind tunnel at the Energy Systems and Turbomachinery Laboratory—University of Bergamo (Bergamo, Italy) (Figure 1) on a six high-pressure turbine nozzle vane cascade whose geometry is typical of a modern heavy-duty gas turbine (Zweifel coefficient of 1.18). The pitch to chord ratio is s/C = 1.04 and the aspect ratio is H/C = 0.69. The flow turning angle at design point is 73.5°. The cascade was tested at an exit Mach number of Ma_{2is} = 0.40 (Re_{2is} = 1.19 × 10^6). A 9% inlet turbulence intensity (Tu_1) level at the vane leading edge plane was obtained by installing a turbulence generator in the wind tunnel admission section. Cascade operating conditions were controlled through inlet total and static pressure and exit static pressure (X/C_{ax} = 1.45). Inlet total pressure and static pressure were measured in the admission section by a three-hole probe located at 1.6 C_{ax} upstream of the leading edge plane. At the same location, inlet boundary layer and turbulence intensity were also measured by means of a flattened Pitot tube and a hot-wire single wire probe (Figure 2). The numerical integration of the autocorrelation function of the acquired hot-wire signal yielded an integral length scale Λ_x of 14.9 mm. The following uncertainties were computed, based on a 95% confidence interval: ±0.3% for Tu_1, ±0.001 for the Mach number and ±0.2 m/s as a maximum for the inlet boundary layer velocity profile.

Four staggered rows of D = 1.0 mm diameter cylindrical holes were designed to cool the leading edge of the three central vanes (Figure 3). The stagnation point is located on the showerhead region between the second and the third row of holes. Each row is composed of 16 cooling holes. Within each row, the hole-to-hole pitch is 5.9D and the hole length is 2.9D. Holes are spread over 90% of the vane height and angled at 45° to the surface. A secondary air supply system was used to feed the cooled vanes, providing a blowing ratio of BR = 3.0. The coolant injection condition was controlled through the monitoring of coolant mass flow and of the corresponding total pressure and temperature in the plenum inside of the vanes. The injected mass flow was measured by an orifice device ($\delta m = \pm 2\%$). BR was computed from coolant to mainstream mass flow MFR = 1.15% and area ratios.

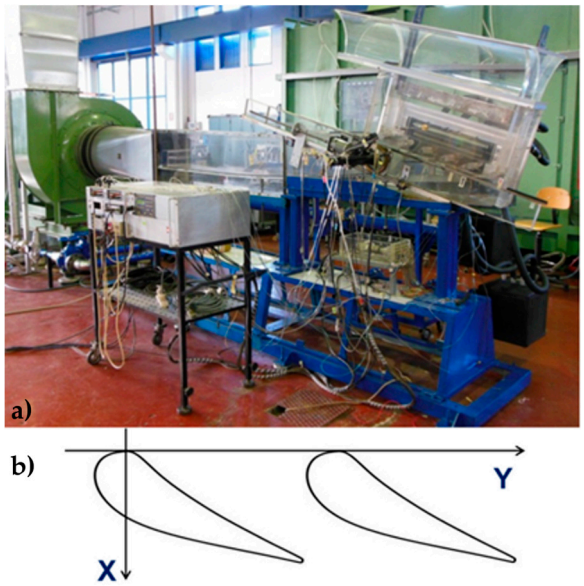

Figure 1. (**a**) View of the wind tunnel; (**b**) cascade model.

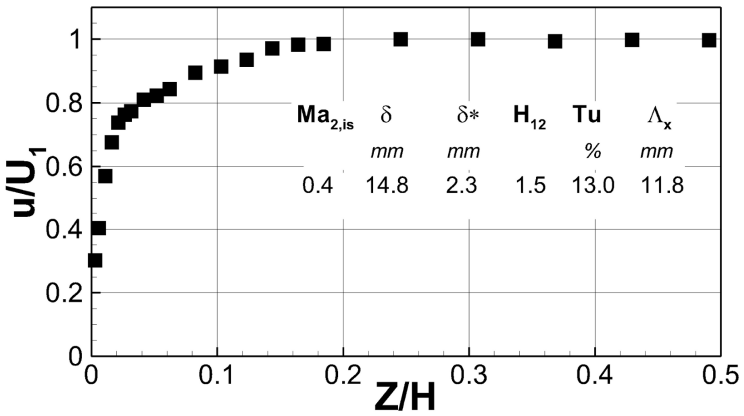

Figure 2. Inlet boundary layer profile ($X/C_{ax} = -1.6$).

The hot streak generator consisted in metal and electrical resistance heating elements. It was located upstream of the test section and provided a ratio of highest temperature in hot streak to main stream temperature of $T_{max,HS}/T_{t\infty}$ = 1.04 at 1 C_{ax} upstream of the vane (Figure 4). The generated inlet temperature distribution across the span is similar to those tested by Barringer et al. in their investigation on temperature inlet profile migration across a high-pressure nozzle vane cascade [13]. The inlet core flow is hot enough to preserve its content while being transported across the passage, even downstream of the cascade. The core of the hot streak was located at about 50% of span;

its tangential position was adjusted at 0% of pitch (Y/s = 0, the hot streak core is aligned to impinge on the vane leading edge, i.e., vane center) and 45% of pitch (Y/s = 0.45, passage center). The inlet temperature distortion extended over two vane pitches in the circumferential direction. A calibrated T-type thermocouple was automatically traversed over a 2D grid at two axial planes: one C_{ax} upstream of the vane, to characterize the 2D inlet temperature field of Figure 4, and one C_{ax} downstream of the vane, to document the hot streak attenuation across the passage. The uncertainty in the measured temperature value was about 0.2 °C.

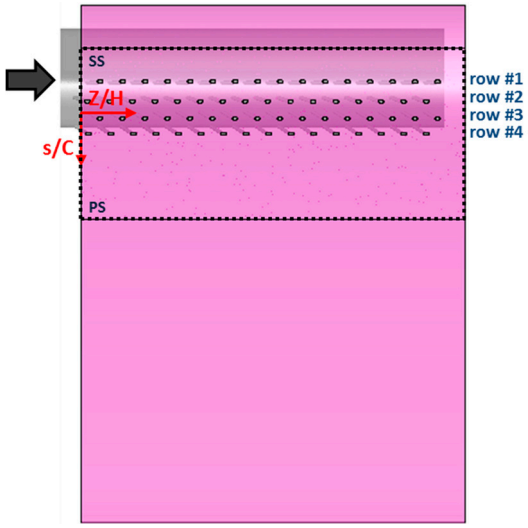

Figure 3. Showerhead geometry with plenum.

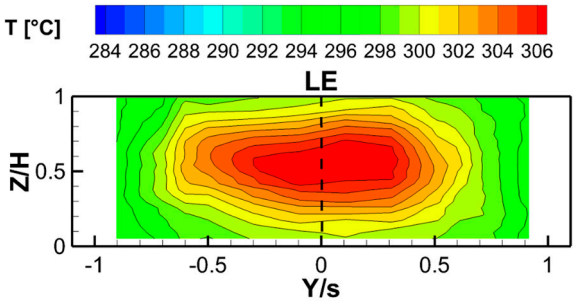

Figure 4. Inlet temperature field (X/C_{ax} = −1.0).

3. Numerical Setup

Steady, adiabatic simulations were performed by employing the ANSYS Fluent code (Canonsburg, PA, USA). The numerical domain needed to contain three vane passages (Figure 5) to handle with an inlet non-uniformity extending over two vane pitches. An unstructured, multi-block, polyhedral mesh was used to discretize the domain. Detailed features of the computational mesh for a single passage can be found in a previous study by Ravelli and Barigozzi [14]. The mesh for the cooled vane configuration (see the central passage in Figure 5) was composed of 67 blocks: one coolant plenum, 64 cooling channels of showerhead type, one block surrounding the leading edge, over a range of s/C = −0.11 on the suction side to s/C = 0.26 to the pressure side, to control the local mesh refinement, and one block for the remaining part of the vane passage. The analysis of mesh sensitivity was based on laterally-averaged film cooling effectiveness values (η_{av}) in the leading edge region (Figure 6), under the assumption of uniform inlet temperature. The number of cells in the leading edge block was progressively increased while coarsening the grid downstream of the vane so as to keep the total

number of grid cells under 19 million. Outside the leading edge block, the mesh was simply extruded in the spanwise direction, with a constant cell size. Grid #1, consisting of 18.48 million cells, resulted to be sufficient for Reynolds-averaged Navier-Stokes (RANS) computations at BR = 3.0. The averaged non-dimensional wall distance, y^+ in the showerhead region within $-0.048 < s/C < 0.059$, is 3.4. For the solid vane configuration, the layout of grid #1 was modified by deleting the coolant plenum and the showerhead cooling channels, thus, the total number of cells was significantly reduced (6.35 million cells). In so doing, the mesh in the vane passage and its refinement in the leading edge block are the same for both configurations, i.e., with and without showerhead film cooling. Actually, three cooled vane passages would have exceeded the memory limit for post-processing.

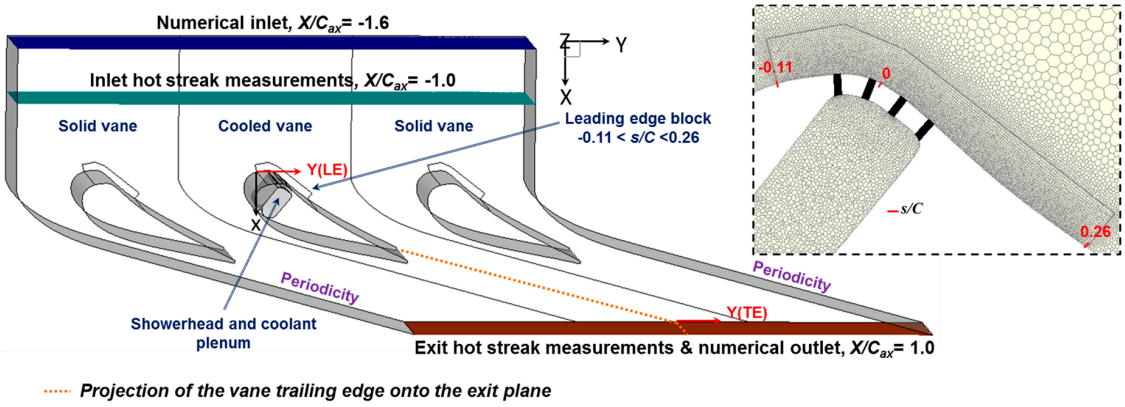

Figure 5. Simulated three-passage vane cascade with hot streak inlet/outlet plane and cross-section view of the mesh in the leading edge region.

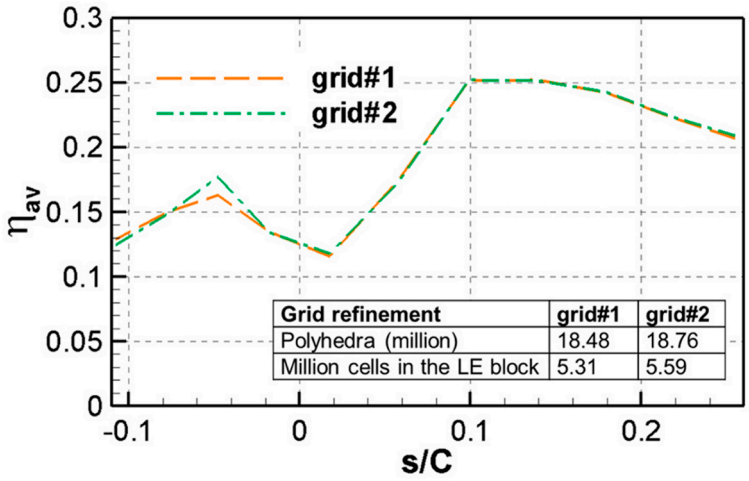

Figure 6. Example of grid resolution test at blowing ratio BR = 3. Shear stress transport (SST) kω predictions of laterally-averaged film cooling effectiveness (η_{av}).

The inlet of the passage was located 1.6 C_{ax} upstream of the vane leading edge. The outlet was located 1 C_{ax} downstream of the vane trailing edge. The boundary conditions prescribed total pressure for the mainstream and static pressure at the outlet (87.9 kPa), in order to assure Ma_{2is} of 0.40. The inlet boundary layer taken from the experiments (Figure 2) was imposed in terms of total pressure profile at the mainstream inlet. An inlet turbulence intensity of Tu_1 = 13%, coupled with Λ_x = 14.9 mm, was set at the inlet of the passage to obtain the Tu_1 level of 9% at the leading edge plane, in agreement with the measured Tu_1 decay reported in Figure 7. It should be pointed out that the measured Tu_1 decay downstream of the turbulence generator compares well with a typical correlation for turbulence decay downstream of cylindrical rods. The inlet profiles of total temperature,

at $X/C_{ax} = -1.6$, was specified to match the measured temperature field at $X/C_{ax} = -1.0$ (Figure 4). The plenum inlet coolant mass flow rate corresponded to the *BR* value of 3.0. Both mainstream and coolant flow were assumed to be air whose total temperature was set at $T_{t\infty} = 295$ K and $T_{tc} = 273$ K, respectively. The 3D Navier–Stokes equations were solved for compressible flow assuming the ideal gas law for the equation of state. Among the most widely used turbulence models for industrial applications, both realizable k-ε and shear stress transport (SST) k-ω with enhanced wall treatment were used for running several simulation sets. The former was definitely chosen to provide closure in the current study since it is better than the latter at predicting film cooling effectiveness, despite some limitations along the suction side of the vane [14].

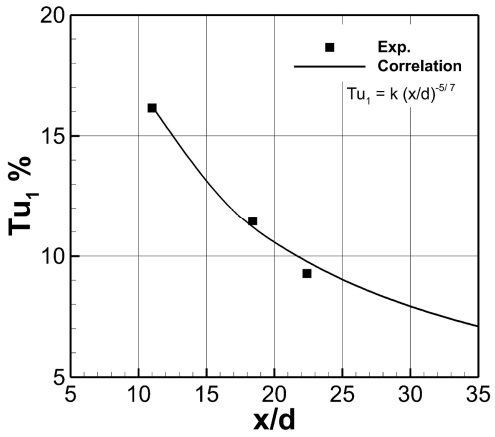

Figure 7. Inlet turbulence intensity (Tu_1) decay.

4. Results and Discussion

Hot streak validation study was performed for the uncooled vane by comparing measured and predicted temperature fields at the vane exit, for two circumferential positions relative to the vane. Moreover, results from the cooled vane simulations with vane aligned hot streak are presented with the aim of assessing the influence of showerhead film cooling on hot streak attenuation.

4.1. Hot Streak Migration without Film Cooling

Hot streak transport mechanism in a stator row is important for heat transfer to the vane and the downstream rotor blade. In Figure 8 measured and predicted temperature distributions at the vane exit ($X/C_{ax} = 1.0$) are placed side by side, for the hot streak core aligned with the vane leading edge (left) or passage center (right). It should be noted that the origin of *Y* coordinate on the exit plane corresponds to a streamline originating from the trailing edge of the central vane, as shown in Figure 5. Negative and positive *Y/s* values refer to the suction side and pressure side of that vane, respectively.

Taking as a reference the inlet temperature distribution of Figure 4, a significant decrease in the hot streak peak temperature is evident from the experiments, whatever the hot streak peak position: the non-dimensional temperature ratio $T_{max,HS} = 307$ K$/T_{t\infty} = 295$ K reduces from 1.04, at the inlet, to 1.005 at the exit plane. Simulations computed realistic static temperature fields at the outlet and accurate hot streak attenuation across the passage. The hot streak development was also well captured in terms of distortion of temperature profiles, due to the interaction of the inlet flow with the vane boundary layer and wake. A negligible peak temperature difference appears when comparing results from impacting and non-impacting hot streaks. This is in agreement with previous findings from both experimental [10] and computational [15] investigations. However, a slightly larger spreading of the hot streak in the tangential direction can be noticed for the vane-aligned case, thus suggesting the potential of increased dispersion of the hot-streak due to boundary layer and wake effects. When referring to

temperature iso-lines, a discrepancy between the experimental and the numerical pattern might be related to the grid spatial discretization, which is much thinner for the simulations.

The total temperature (T_t) contours shown at the bottom of Figure 8 are useful to identify the hot core downstream location, together with its pitchwise and spanwise extension. Outside of the hot streak induced flow perturbation, the T_t value of 295 K is unaltered through the vane passage.

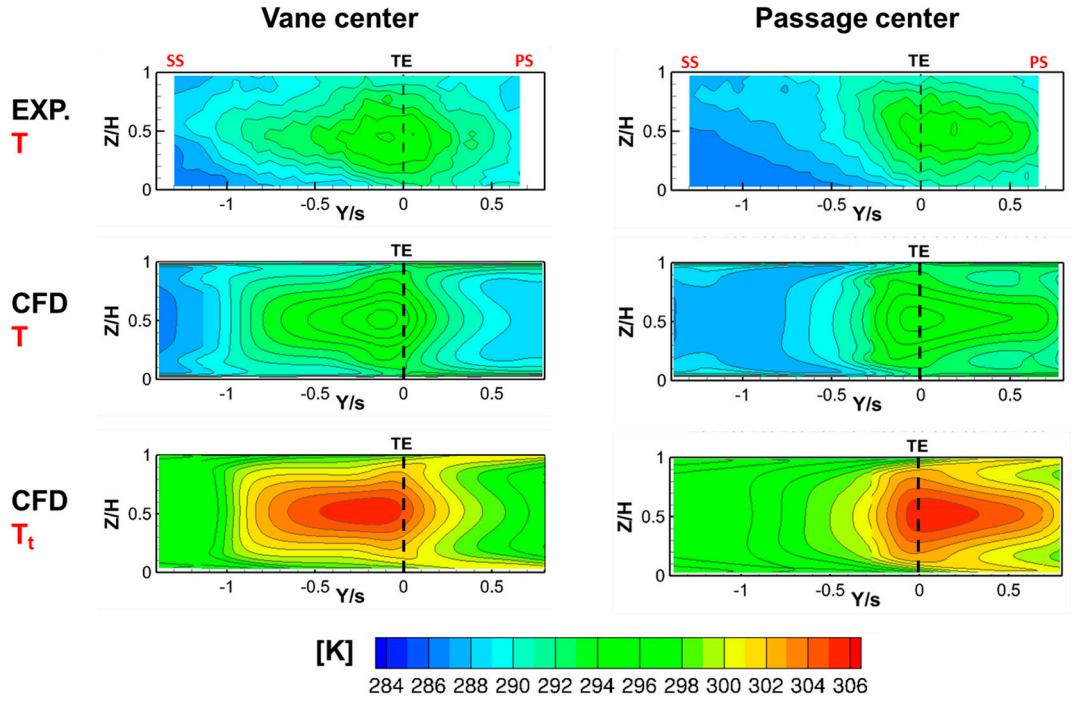

Figure 8. Comparison between experimental and predicted temperature fields at the vane exit plane (X/C_{ax} = 1.0) for the hot streak aligned with the vane or passage center. CFD: computational fluid dynamics.

Hot streak interaction with the vanes of the simulated cascade can be discussed looking at Figure 9, where contours of the normalized ratio Θ_{HS} and Θ_{HSt} are shown at the midspan plane. Figure 10 reports the evolution of Θ_{HS} along each vane. With the hot streak aligned with the (central) vane, the core of the hot spot travels in the axial direction and impacts the pressure side of the leading edge, where the stagnation point is located. Moving downstream along the pressure side of the vane, the strength of the hot streak is well preserved up to the trailing edge (Θ_{HS} = 0.89 at X/C_{ax} = 0.9). Conversely, the strong acceleration of the flow, favored by the blunt leading edge, causes noticeable hot streak attenuation along the upper part of the suction side: this translates into the lowest Θ_{HS} of 0.74 at X/C_{ax} = 0.31 (see vane center #2 in Figure 10). Experimental data presented in [10] show similar trends of hot streak attenuation: the greatest reduction of the peak temperature on the suction side occurred around the first third of the suction side length. In addition, lower rate of attenuation was found on the pressure side, as compared to the suction side. For this hot streak position, it is obvious that the highest levels of Θ_{HS} are reported for the central vane (#2). However, vane #1 is also affected by the hot streak, especially on the pressure side, where Θ_{HS} reaches the maximum of 0.16 at X/C_{ax} = 0.72. The profile of Θ_{HS} for vane #3 is representative of undisturbed inlet flow.

When the hot streak core is positioned at mid-passage, the hot core is responsible for increasing the pressure side surface temperature of vane #2 up to Θ_{HS} = 0.8 at X/C_{ax} = 0.3. The periphery of the inlet temperature distortion reaches the leading edge of vane #3 (Θ_{HS} = 0.53) and travels along both sides of the vane subject to moderate attenuation: the minimum Θ_{HS} value is 0.37 at X/C_{ax} = 0.3, on the suction side. Conversely, Θ_{HS} profile for vane #1 comes back to the undisturbed inlet flow case.

The additional information provided by Θ_{HSt} contours deals with the downstream travelling of the high temperature region. For the vane center alignment, it is divided into two parts by vane #2: at increasing axial locations, it is pressed to the wall at the pressure side, whereas it becomes slightly wider in the tangential direction along the suction side, consistently with findings in [15]. For the passage center alignment, the high temperature region gets squeezed between vane #2 and #3: at the trailing edge, it situates close to the pressure side of vane #2.

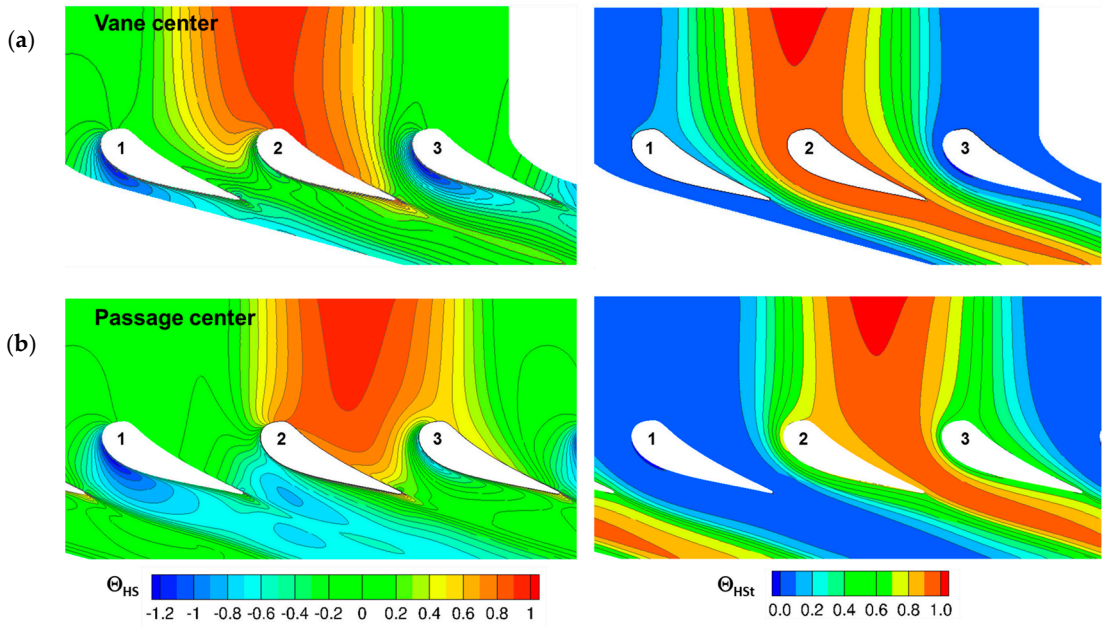

Figure 9. Predicted temperature ratio (Θ_{HS} and Θ_{HSt}) at midspan (Z/H = 0.5) for the hot streak aligned with the vane (**a**) or passage center (**b**).

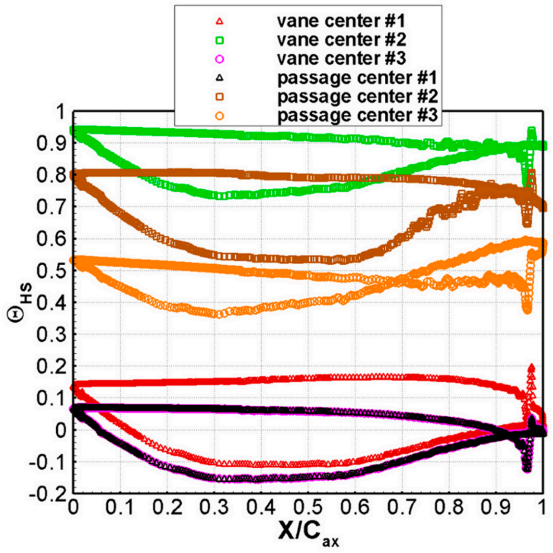

Figure 10. Predicted temperature ratio (Θ_{HS}) around each vane at midspan (Z/H = 0.5) for the hot streak aligned with the vane or passage center.

4.2. Hot Streak Migration with Film Cooling

The interaction of the hot streak with the coolant exiting the showerhead was numerically assessed for the vane center alignment at blowing ratio of BR = 3.0 (MFR = 1.15%), i.e., a trade-off between

cooling air consumption and cooling efficiency around the leading edge region [14]. A comparison of the simulated thermal profiles with no blowing and with showerhead injection is presented in Figure 11, along a midspan traverse extending normal the vane surface, at the trailing edge. The reduction in the peak Θ_{HS} value from 0.89 to 0.77 indicates that showerhead film cooling is responsible for a hot streak attenuation of about 13% at the vane trailing edge (Y/s = 0). As expected, the reported Θ_{HS} profiles overlay moving away from the trailing edge. Indeed, the additional attenuation of the hot streak due to showerhead injection is known to be moderate at downstream locations [10]. The discussion gets a lot more interesting when it comes to coolant interaction with the hot streak within the leading edge region. The core of the hot streak is directed onto the showerhead (Figure 12) but the hot gas is prevented from impacting the vane surface on either side of the stagnation point, thanks to a protective layer of coolant flowing next to the vane. This thermal protection is more effective on the pressure side, as compared to suction side, where jet dissipation is enhanced by the mixing with the accelerating hot mainstream. Conversely, the hot gas is able to impact directly on the stagnation point and penetrate in between the showerhead rows of the cooling holes. Nevertheless, the hot streak effects, which are somewhat mitigated in the front part of the vane due to film cooling, lead to a significant increase in surface temperature in the rear part of the vane, in agreement with [12]. It becomes evident from Figure 12 that the lower-rear part of the pressure side is exposed to hot flow, with no coolant coverage.

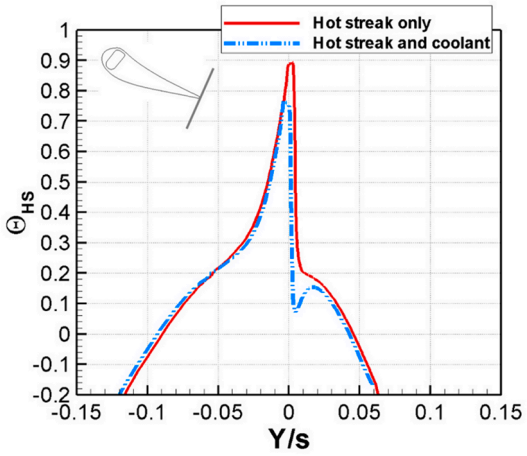

Figure 11. Predicted midspan temperature ratio (Θ_{HS}) at the trailing edge, for the hot streak aligned with the vane.

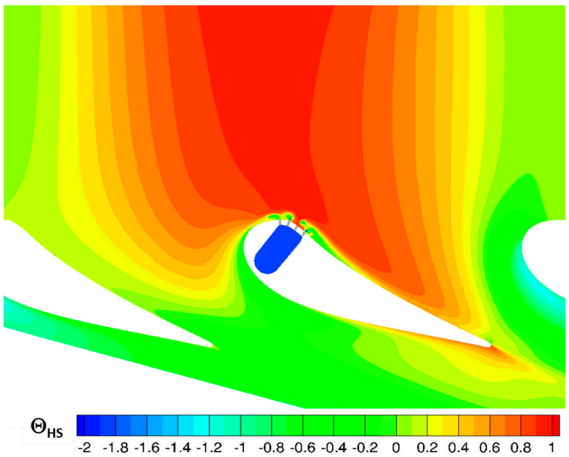

Figure 12. Predicted temperature ratio (Θ_{HS}) at midspan (Z/H = 0.5) for the hot streak aligned with the vane, combined with showerhead film cooling (blowing ratio BR = 3.0, coolant-to-mainstream mass flow ratio MFR = 1.15%).

With a focus on the vane leading edge, i.e., where showerhead film cooling plays a relevant role in hot streak attenuation, the simulations were used to evaluate the applicability of the superposition principle. Taking inspiration from [11], hot streak reduction due to film cooling was estimated starting from independent hot streak and film cooling results, according with the following:

$$\left\{\frac{T-T_{t\infty}}{T_{\max,HS}-T_{t\infty}}\right\}_{Superposition}=\left\{\frac{T-T_{t\infty}}{T_{\max,HS}-T_{t\infty}}\right\}_{Hot\ streak\ only}+\left\{\frac{T-T_{t\infty}}{T_{\max,HS}-T_{t\infty}}\right\}_{Coolant\ only} \quad (1)$$

$$\{\Theta_{HS}\}_{Superposition}=\{\Theta_{HS}\}_{Hot\ streak\ only}+\{\Theta_{HS}\}_{Coolant\ only}$$

Equation (1) is valid under the assumptions of constant specific heat and density, as well as the invariant velocity for a given position. The latter requirement is fully respected since the hot streak does not modify streamline flow pattern in a vane passage. The former condition is satisfied in flows at low Mach number, such as that around the leading edge, subject to small variation in temperature (±25 K). The load profile shown in Figure 13 indicates that the stagnation point is slightly shifted to the pressure side. A strong acceleration occurs along the suction side, due to the blunt leading edge. Conversely, the Mach number distribution varies smoothly along the pressure side, with progressively increasing flow acceleration up to the trailing edge. In the showerhead region, the hypothesis of constant density is validated by Ma_{is} values below 0.2.

Figure 14a,b show the computed surface distribution of Θ_{HS} in the leading edge region for hot streak alone and coolant alone. These distributions were used to compute the superposition Θ_{HS} contours according with Equation (1) (Figure 14c).

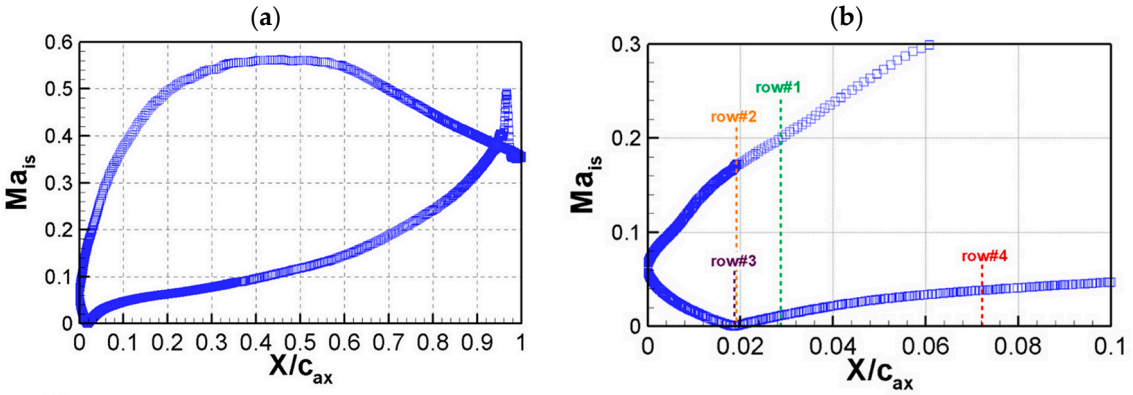

Figure 13. Isentropic Mach number (Ma_{is}) distribution at midspan (Z/H = 0.5) (**a**) with zoomed-in view on vane leading edge (**b**).

The comparison of the superposition results against those obtained from the simulation of combined hot streak and showerhead film cooling (Figure 14d) allowed estimating the spatial contour of the error (Figure 14e) as:

$$\Delta\% = \left(\frac{\{\Theta_{HS}\}_{Superposition}-\{\Theta_{HS}\}_{Hot\ streak\&coolant}}{max(\Theta_{HS})-min(\Theta_{HS})}\right)\times 100 \quad (2)$$

Starting from Figure 14a, the thermal footprint of the hot streak on the leading edge reveals the presence of a hot core (Θ_{HS} = 0.94) located in a narrow area around midspan (0.4 < Z/H < 0.6). Θ_{HS}, being almost symmetrically distributed with respect to mid span, is reduced to 0.53 at both the tip and hub of the vane. Moving to the results from the "coolant only" case of Figure 14b, the lower the Θ_{HS} value the more effective the thermal coverage. The coolant accumulation toward the tip in the jet exit direction causes a continuous reduction in Θ_{HS} at increasing Z/H. In the central section of the vane span (0.2 < Z/H < 0.9), the pressure side is characterized by oblique travelling of the coolant, especially evident at s/C > 0.1. However, merging of coolant jets exiting row #3 and #4 helps obtaining

spanwise uniformity and values of Θ_{HS} as low as -0.82 in the region within $0.04 < s/C < 0.1$. On the suction side the lowest levels of Θ_{HS} (-1.05) are located toward the tip, immediately downstream of row #1. Along the stagnation line values of Θ_{HS} close to zero denote poor cooling performance. Following the lesson learnt from [14], the largest percent error, between the experimental and the computed Θ_{HS} values, occurs in the proximity of row #1, where the interaction of the coolant with the accelerating mainstream puts a strain on the steady RANS approach. Predictions of Θ_{HS} get more accurate around the stagnation line and along the pressure side. The point is that showerhead film cooling jets, being completely separated from the vane surface even at relatively low blowing ratios, are challenging for numerical modelling. In addition, turbulence in the leading edge region is highly anisotropic, in contrast to the isotropy Boussinesq assumption. Figure 14d shows evidence that the hot streak reduction due to film cooling is almost negligible at stagnation line, especially around midspan where Θ_{HS} gets the peak of 0.83. High Θ_{HS} values extend also in between the pressure side and the suction side rows of holes. Conversely, except for the region close to the hub ($Z/H < 0.2$), mixing with coolant produces remarkable hot streak attenuation at $s/C < -0.06$, where the highest Θ_{HS} was found to be 0.32. On the pressure side, outside the showerhead, Θ_{HS} values are around zero or slightly negative, but higher than those of the "coolant only" case. This means that coolant is still providing some protection, thanks to high persistence of the pressure side cooling jets. It becomes evident from Figure 14c–e that the superposition results match quite well those from the combined hot streak and film cooling simulation. Error was kept within $\Delta = \pm 8\%$ over the showerhead region, i.e., in between the rows of cooling holes. Along the suction side, at $s/C < -0.06$, superposition over predicts the benefit of coolant in reducing the vane surface temperature in between the cooling jets, toward the tip (minimum Δ of -9.5%), and under predicts the hot streak reduction along the path of the coolant flow exiting row#1 (maximum Δ of 12%). This might be due to the fact that the superposition principle does not take into account the influence of local, strong temperature gradients in the flow due to coolant/hot streak interaction, as suggested in [11]. On the pressure side, the computed error falls within an acceptable range ($\Delta = \pm 10\%$) in the central section of the vane ($0.2 < Z/H < 0.8$), where side walls effects on coolant flow are negligible.

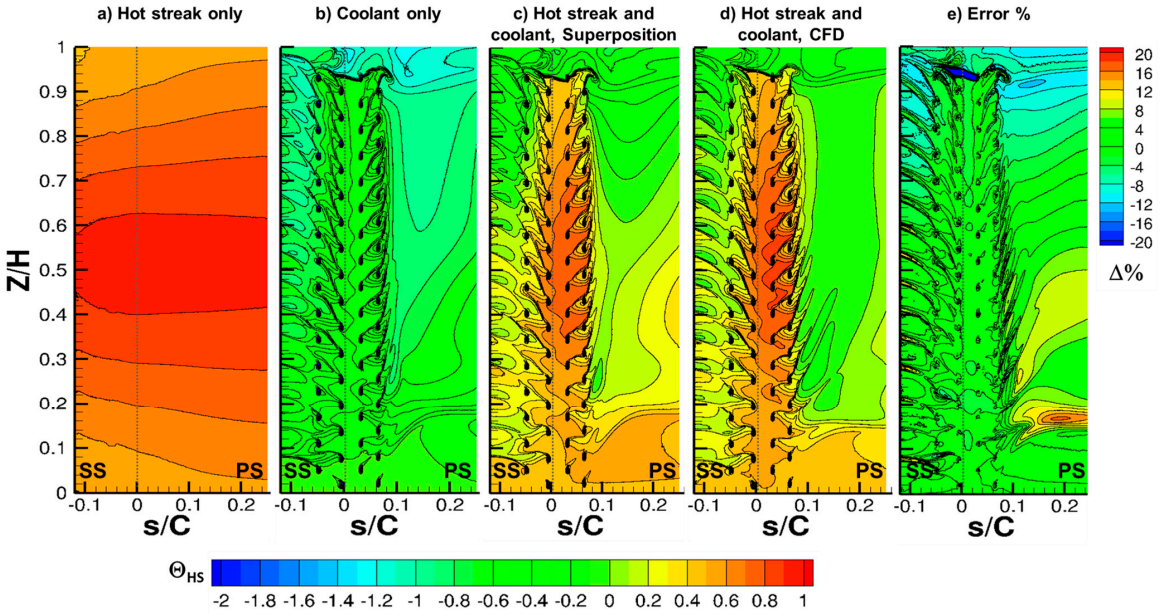

Figure 14. Comparison of predicted and superposition temperature ratio (Θ_{HS}) for the vane-aligned hot streak, combined with showerhead blowing at BR = 3.0 (MFR = 1.15%). (**a**) Hot streak only; (**b**) coolant only; (**c**) superposition of hot streak and coolant; (**d**) CFD modelling of hot streak and coolant; (**e**) error (%).

5. Conclusions

Steady simulations and thermal measurements were used to examine hot streak migration in a high-pressure turbine vane cascade with showerhead film cooling, under conditions of compressible flow and high inlet turbulence. Validation was performed through a comparison of predicted and measured thermal fields at the exit of the passage, with no blowing, for two hot streak circumferential positions relative to the vane. Clocking effects of inlet temperature non-uniformity on hot streak attenuation were found to be negligible for the uncooled vane: in fact, positioning the hot streak core at the leading edge or at the mid passage did not change the peak temperature reduction, from $T_{max,HS}/T_{t\infty}$ = 1.04, at the inlet, to $T_{max,HS}/T_{t\infty}$ = 1.005, at the outlet.

Once the computational fluid dynamics (CFD) model has been validated, the leading edge aligned configuration was numerically investigated subject to showerhead blowing (BR = 3.0, MFR = 1.15%). On the one hand, the additional attenuation of the hot streak due to showerhead film cooling appeared moderate at the vane exit. On the other hand, vane surface temperature in the leading edge region was strongly affected by coolant jet interaction with the approaching head-on hot spot. The stagnation line was exposed to the highest (normalized) temperature, whereas significant hot streak reduction was found outside the showerhead, especially on the pressure side. Finally, the superposition method proved to be fairly capable of predicting hot streak mixing with coolant on the simulated leading edge of a gas turbine vane.

Acknowledgments: The authors gratefully acknowledge the Italian Ministry of Instruction, University and Research (MIUR) for funding this research project (PRIN2010-2011). Moreover, this work has been supported by CINECA Consortium through an ISCRA (Italian Super Computing Resource Allocation) 2015 grant.

Author Contributions: Giovanna Barigozzi conceived and performed the experimental tests, with the practical help of Silvia Mosconi. Antonio Perdichizzi supervised the whole process. Silvia Ravelli ran the CFD simulations and wrote most of the paper.

Conflicts of Interest: The authors declare no conflict of interest.

Nomenclature

$A_c = N\pi D^2/4$	Hole cross-section
$A_\infty = 0.9Hs$	Vane channel cross-section
$BR = MFR\ A_\infty/A_c$	Blowing ratio
C	Vane chord
d	Rod diameter
D	Hole diameter
H	Vane height
Ma	Mach number
$MFR\% = m_c/m_\infty$	Coolant-to-mainstream mass flow ratio
N	Number of showerhead holes
$Re_{2is} = U_{2is}c/\nu$	Isentropic outlet Reynolds number
s	Vane pitch/Curvilinear coordinate
T	Temperature
Tu	Turbulence intensity level
X,Y,Z	Coordinate system
Δ	Error
Λ	Length scale
$\eta = (T_{aw} - T_\infty)/(T_c - T_\infty)$	Film cooling effectiveness
$\Theta_{HS} = (T - T_{t\infty})/(T_{\max,HS} - T_{t\infty})$	Normalized temperature ratio
$\Theta_{HSt} = (T_t - T_{t\infty})/(T_{\max,HS} - T_{t\infty})$	Normalized temperature ratio
ν	Kinematic viscosity
Subscripts	
1	Inlet
2	Exit

av	Laterally averaged
ax	Axial
aw	Adiabatic wall
c	Cooling flow
is	Isentropic condition
HS	Hot streak
max	Maximum
min	Minimum
w	Wall
∞	Free stream

References

1. Butler, T.L.; Sharma, O.P.; Joslyn, H.D.; Dring, R.P. Redistribution of an Inlet Temperature Distortion in an Axial Flow Turbine Stage. *J. Propuls. Power* **1989**, *5*, 64–71. [CrossRef]
2. Hermanson, K.S.; Thole, K.A. Effect of Nonuniform Inlet Conditions on Endwall Secondary Flows. *J. Turbomach.* **2002**, *124*, 623–631. [CrossRef]
3. Barringer, M.; Thole, K.A.; Polanka, M.D. An Experimental Study of Combustor Exit Profile Shapes on Endwall Heat Transfer in High Pressure Turbine Vanes. *J. Turbomach.* **2009**, *131*, 021009. [CrossRef]
4. Povey, T.; Chana, K.S.; Jones, T.V.; Hurrion, J. The Effect of Hot-Streaks on HP Vane Surface and Endwall Heat Transfer: An Experimental and Numerical Study. *J. Turbomach.* **2005**, *129*, 32–43. [CrossRef]
5. Qureshi, I.; Beretta, A.; Povey, T. Effect of Simulated Combustor Temperature Nonuniformity on HP Vane and Endwall Heat Transfer: An Experimental and Computational Investigation. *J. Eng. Gas Turbines Power* **2010**, *133*, 031901. [CrossRef]
6. Mathison, R.M.; Haldeman, C.W.; Dunn, M.G. Aerodynamics and Heat Transfer for a Cooled One and One-Half Stage High-Pressure Turbine—Part I: Vane Inlet Temperature Profile Generation and Migration. *J. Turbomach.* **2011**, *134*, 011006. [CrossRef]
7. Ong, J.; Miller, R.J. Hot streak and vane coolant migration in a downstream rotor. *J. Turbomach.* **2012**, *134*, 051002. [CrossRef]
8. Basol, A.M.; Jenny, P.; Ibrahim, M.; Kalfas, A.I.; Abhari, R.S. Hot Streak Migration in a Turbine Stage: Integrated Design to Improve Aerothermal Performance. *J. Eng. Gas Turbines Power* **2011**, *133*, 061901. [CrossRef]
9. Regina, K.; Basol, A.M.; Jenny, P.; Kalfas, A.I.; Abhari, R.S. Hot Streak Shaping and Migration in an Axial Turbine. *Int. J. Gas Turbine Propuls. Power Syst.* **2013**, *5*, 30–36.
10. Jenkins, S.C.; Varadarajan, K.; Bogard, D.G. The Effects of High Mainstream Turbulence and Turbine Vane Film Cooling on the Dispersion of a Simulated Hot Streak. *J. Turbomach.* **2004**, *126*, 203–211. [CrossRef]
11. Jenkins, S.C.; Bogard, D.G. Superposition Predictions of the Reduction of Hot Streaks by Coolant from a Film-Cooled Guide Vane. *J. Turbomach.* **2009**, *131*, 041002. [CrossRef]
12. Griffini, D.; Insinna, M.; Salvadori, S.; Martelli, F. Clocking Effects of Inlet Nonuniformities in a Fully Cooled High-Pressure Vane: A Conjugate Heat Transfer Analysis. *J. Turbomach.* **2015**, *138*, 021006. [CrossRef]
13. Barringer, M.; Thole, K.A.; Polanka, M.D.; Clark, J.P.; Koch, P.J. Migration of Combustor Exit Profiles Through High Pressure Turbine Vanes. *J. Turbomach.* **2009**, *131*, 021010. [CrossRef]
14. Ravelli, S.; Barigozzi, G. Comparison of RANS and Detached Eddy Simulation Modeling Against Measurements of Leading Edge Film Cooling on a First-Stage Vane. *J. Turbomach.* **2017**, *139*, 051005. [CrossRef]
15. An, B.-T.; Liu, J.-J.; Jiang, H.-D. Numerical Investigation on Unsteady Effects of Hot Streak on Flow and Heat Transfer in a Turbine Stage. *J. Turbomach.* **2009**, *131*, 031015. [CrossRef]